Research Article

Atila Poro, Mark G. Blackford, Fatemeh Davoudi, Amirreza Mohandes, Mohammad Madani, Samaneh Rezaei, and Elnaz Bozorgzadeh

The New Ephemeris and Light Curve Analysis of V870 Ara by the Ground-Based and TESS Data

https://doi.org/10.1515/astro-2021-0004
Received Mar 31, 2021; accepted Jul 6, 2021

Abstract: New CCD photometric observations and their investigation of the W UMa-type binary, V870 Ara, are presented. Light curves of the system were taken through *BVI*filters from the Congarinni Observatory in Australia. The new ephemeris is calculated based on seven new determined minimum times, together with the TESS data and others compiled from the literature. Photometric solutions determined by the Wilson-Devinney (W-D) code are combined with the Monte Carlo simulation to determine the adjustable parameters' uncertainties. These solutions suggest that V870 Ara is a contact binary system with a mass ratio of 0.082, a fillout factor of 96±4 percent, and an inclination of 73.60±0.64 degrees. The absolute parameters of V870 Ara were determined by combining the Gaia EDR3 parallax and photometric elements.

Keywords: techniques: photometric - binaries: eclipsing - stars: individual (V870 Ara)

1 Introduction

The contact binary system V870 Ara is located in the southern constellation Ara and has a magnitude of $V = 8.96$ and an orbital period of 0.399722 day (Eker et al. 2009; Szalai et al. 2007). V870 Ara is one of the systems discovered by the Hipparcos space-based telescope. Kazarovets et al. (1999) put this star in the Hipparcos variable stars' catalog and suggested that V870 Ara may be a Delta Scuti variable star. Selam (2004) analyzed the light curve of this system for the first time, calculated a mass ratio of $q = 0.25$, and put this variable star in the W-subtypes of the W UMa contact binary type. Szalai et al. (2007) spectroscopically measured $q = 0.082 \pm 0.030$and computed this system's distance to be 112.5 parsecs. Szalai et al. (2007) and Pribulla and Rucinski (2014) studied the period change of five systems, including the V870 Ara, to identify the third body, and they could not find signs of multiplicity in the V870 Ara. Ulaş et al. (2012) classified the V870 Ara as a late-type contact binary system, whereas Hu et al. (2018) classified it as a deep-contact binary system.

In this study, the multi-color CCD light curves in B, V, and I bands, along with photometric data obtained from the TESS space telescope, are presented. We extracted the minimum times based on the Monte Carlo Markov Chain (MCMC) method and then determined a new ephemeris for this binary system. The light curve solution with the W-D code combined with the Monte Carlo (MC) simulation was performed. Absolute parameters of the system were derived.

2 Observation and Data Reduction

The new photometric observations of V870 Ara in June 2020 were made using *BVI* standard filters. These observations were carried out with the Orian ED80T CF refractor telescope at the Congarinni Observatory, located in Australia (152° 52′ E and 30°44′ S). A total of 1480 photos in the filters were taken by a CCD Atik One 6.0. This CCD has 2750×2200 pixels, 4.54-micron square, and we used 1 × 1 binning for observations. The temperature of the CCD is set at −10°C. In these observations, we selected a comparison star and a check star close to the V870 Ara. Aspects like apparent magnitude, spectral category, and distance from V870 Ara were taken into account when choosing the comparison and the check stars. The characteristics of all these stars are shown in Table 1, and the field of view is shown in Figure 1. MaxIm DL software was used to apply dark, bias, and flat-field corrections and perform aperture photometry.

Atila Poro, Fatemeh Davoudi, Amirreza Mohandes, Mohammad Madani, Samaneh Rezaei, Elnaz Bozorgzadeh The International Occultation Timing Association Middle East section, Iran, E-mail: info@iota-me.com

Mark G. Blackford Variable Stars South (VSS), Congarinni Observatory, Congarinni, NSW, 2447, Australia

Table 1. Characteristics of the binary system, comparison star, and check star (from Simbad http://simbad.u-strasbg.fr/simbad/).

Type	Name	RA. (J2000)	DEC. (J2000)	*V* (mag.)	Sp. Type
Variable	V870 Ara	18 08 22.6745	−56 46 01.8007	8.96	F7/G0
Comparison	TYC 8751-1567-1	18 11 29.2004	−56 36 55.7000	9.88	G5
Check	TYC 8751-1647-1	18 08 20.7684	−56 45 30.4884	9.84	G5

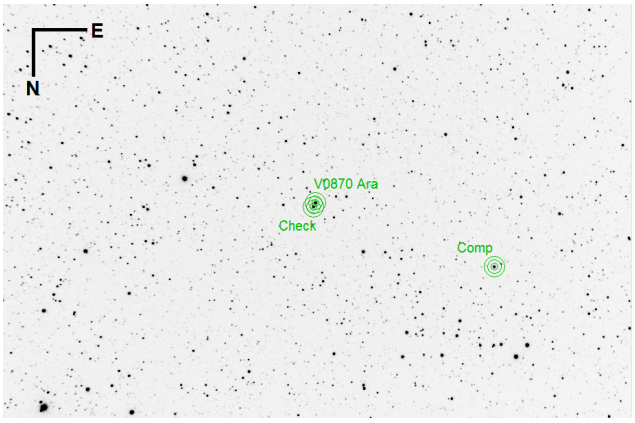

Fig. 1. The position of V870 Ara, TYC 8751-1567-1 (comparison star), and TYC 8751-1647-1 (check star). The field of view is 90 by 72 arcminutes. The circles are only to indicate the position of each star with much larger rings. The aperture radius used for photometry was 8 pixels, gap width 5 pixels and annulus thickness 5 pixels.

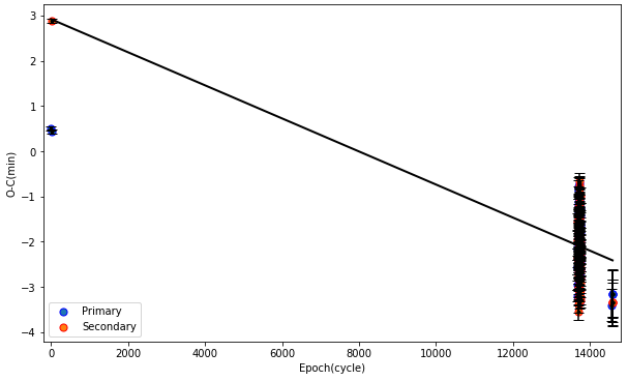

Fig. 2. The O-C diagram of V870 Ara with the linear trend in the data using the MCMC method. The blue color corresponds to primary minima times, while the red color corresponds to secondary minima times.

The Transiting Exoplanet Survey Satellite (TESS) is NASA's two-year mission to search for exoplanets and variable stars and it was launched in 2018. TESS observed V870 Ara (TIC 118271395) from 19 June to 18 July, 2019, and the data is available at the Mikulski Space Telescope Archive (MAST). We extracted TESS style curves detrended by the TESS Science Processing Operations Center (SPOC) pipeline (Jenkins et al. 2016) from the MAST using the LightKurve code https://docs.lightkurve.org/. It was observed in sector 13 by Camera 2 and CCD 4 at a 120 second cadence. The data normalized by the AstroImageJ (AIJ) software (Collins et al. 2017).

3 New Ephemeris

To extract the minimum times and their uncertainties, we employed the Monte Carlo Markov Chain (MCMC) approach through fitting the models to the light curves based on Gaussian distributions (Poro et al. 2020). The PyMC3 package was used to implement the code for this part of the study (Salvatier et al. 2016). According to this, we found four primary and three secondary minima in our observed light curves. Using the same method, we also extracted 135 minimum times from the TESS data. We used a Python code based on the lightKurve package to extract SAP light curves from calibrated TESS data files obtained from the Mikulski Space Telescope Archive (MAST) (Cardoso et al. 2018). All the extracted minima times from our observation and TESS data with the collected minima times from the literature are listed in Table 2. All times of minimum are expressed in Barycentric Julian Date in Barycentric Dynamical Time (BJDTDB) are in column 1, their uncertainties appear in column 2, epochs of these minima times in column 3, O-C values in column 4, and the references to minima times in the last column.

We used the following light elements as the reference ephemeris (Szalai 2007) for computing epoch and initial O-C values in Table 2,

$$Min.I\,(BJD_{TDB}) = 2453185.13865\,(3) + 0.39972200(2) \times E. \quad (1)$$

Table 2. Times of minima of V870 Ara (we ignored the literature's minimum times of three and less than three decimal places to improve accuracy)

Min. (BJDTDB)	Error	Epoch	O-C (day)	Reference	Min. (BJDTDB)	Error	Epoch	O-C (day)	Reference
2453185.13865	0.00003	0	0	Szalai 2007	2458669.52324	0.00014	13720.5	-0.0011	TESS
2453195.13215	0.00003	25	0.0004	Szalai 2007	2458669.72326	0.00011	13721	-0.0010	TESS
2453196.13325	0.00003	27.5	0.0022	Szalai 2007	2458669.92308	0.00013	13721.5	-0.0010	TESS
2458654.13301	0.00007	13682	-0.0020	TESS	2458670.12200	0.00012	13722	-0.0019	TESS
2458654.53294	0.00011	13683	-0.0018	TESS	2458670.32288	0.00013	13722.5	-0.0009	TESS
2458654.53275	0.00011	13683	-0.0020	TESS	2458670.52261	0.00010	13723	-0.0010	TESS
2458654.73291	0.00014	13683.5	-0.0017	TESS	2458670.72266	0.00012	13723.5	-0.0009	TESS
2458654.93253	0.00010	13684	-0.0020	TESS	2458670.92232	0.00009	13724	-0.0011	TESS
2458655.13275	0.00013	13684.5	-0.0016	TESS	2458671.12228	0.00012	13724.5	-0.0010	TESS
2458655.33239	0.00009	13685	-0.0018	TESS	2458671.32220	0.00009	13725	-0.0009	TESS
2458655.53257	0.00013	13685.5	-0.0015	TESS	2458671.52192	0.00012	13725.5	-0.0010	TESS
2458655.73213	0.00009	13686	-0.0018	TESS	2458671.72197	0.00010	13726	-0.0009	TESS
2458655.93237	0.00013	13686.5	-0.0014	TESS	2458671.92165	0.00012	13726.5	-0.0010	TESS
2458656.13197	0.00008	13687	-0.0017	TESS	2458672.12135	0.00011	13727	-0.0012	TESS
2458656.33211	0.00013	13687.5	-0.0014	TESS	2458672.32138	0.00016	13727.5	-0.0010	TESS
2458656.53179	0.00008	13688	-0.0016	TESS	2458672.52056	0.00014	13728	-0.0017	TESS
2458656.73205	0.00013	13688.5	-0.0012	TESS	2458672.72095	0.00015	13728.5	-0.0012	TESS
2458656.93169	0.00010	13689	-0.0014	TESS	2458672.92040	0.00011	13729	-0.0016	TESS
2458657.13105	0.00014	13689.5	-0.0019	TESS	2458673.12083	0.00014	13729.5	-0.0010	TESS
2458657.33159	0.00010	13690	-0.0012	TESS	2458673.32019	0.00010	13730	-0.0015	TESS
2458657.53068	0.00017	13690.5	-0.0020	TESS	2458673.52050	0.00016	13730.5	-0.0011	TESS
2458657.73159	0.00015	13691	-0.0010	TESS	2458673.71996	0.00009	13731	-0.0015	TESS
2458657.93132	0.00015	13691.5	-0.0011	TESS	2458673.92036	0.00013	13731.5	-0.0009	TESS
2458658.13143	0.00012	13692	-0.0008	TESS	2458674.11977	0.00009	13732	-0.0014	TESS
2458658.33008	0.00015	13692.5	-0.0021	TESS	2458674.31996	0.00012	13732.5	-0.0011	TESS
2458658.53068	0.00010	13693	-0.0013	TESS	2458674.51884	0.00009	13733	-0.0020	TESS
2458658.73077	0.00013	13693.5	-0.0011	TESS	2458674.71978	0.00012	13733.5	-0.0010	TESS
2458658.92990	0.00008	13694	-0.0018	TESS	2458674.91918	0.00009	13734	-0.0014	TESS
2458659.13009	0.00012	13694.5	-0.0015	TESS	2458675.11952	0.00012	13734.5	-0.0009	TESS
2458659.32994	0.00009	13695	-0.0015	TESS	2458675.31809	0.00009	13735	-0.0022	TESS
2458659.52971	0.00012	13695.5	-0.0016	TESS	2458675.31909	0.00009	13735	-0.0012	TESS
2458659.72964	0.00009	13696	-0.0015	TESS	2458675.71785	0.00009	13736	-0.0022	TESS
2458659.93006	0.00012	13696.5	-0.0010	TESS	2458675.91889	0.00012	13736.5	-0.0010	TESS
2458660.13001	0.00008	13697	-0.0009	TESS	2458676.11885	0.00009	13737	-0.0009	TESS
2458660.32862	0.00012	13697.5	-0.0021	TESS	2458676.31795	0.00013	13737.5	-0.0017	TESS
2458660.52971	0.00007	13698	-0.0009	TESS	2458676.51852	0.00010	13738	-0.0010	TESS
2458660.72839	0.00012	13698.5	-0.0021	TESS	2458676.71789	0.00012	13738.5	-0.0015	TESS
2458660.92899	0.00011	13699	-0.0013	TESS	2458676.91744	0.00009	13739	-0.0018	TESS
2458661.12883	0.00014	13699.5	-0.0014	TESS	2458677.11781	0.00012	13739.5	-0.0013	TESS
2458661.32794	0.00009	13700	-0.0021	TESS	2458677.31726	0.00008	13740	-0.0017	TESS
2458661.52769	0.00013	13700.5	-0.0022	TESS	2458677.51663	0.00012	13740.5	-0.0022	TESS
2458661.72860	0.00010	13701	-0.0012	TESS	2458677.71703	0.00008	13741	-0.0016	TESS
2458661.92751	0.00013	13701.5	-0.0021	TESS	2458677.91737	0.00012	13741.5	-0.0011	TESS
2458662.12847	0.00008	13702	-0.0010	TESS	2458678.11692	0.00008	13742	-0.0015	TESS
2458662.32739	0.00012	13702.5	-0.0020	TESS	2458678.31603	0.00011	13742.5	-0.0022	TESS
2458662.52812	0.00008	13703	-0.0011	TESS	2458678.51662	0.00008	13743	-0.0015	TESS
2458662.72702	0.00012	13703.5	-0.0021	TESS	2458678.71614	0.00011	13743.5	-0.0018	TESS
2458662.92796	0.00008	13704	-0.0010	TESS	2458678.91643	0.00010	13744	-0.0014	TESS
2458663.12671	0.00013	13704.5	-0.0021	TESS	2458679.11688	0.00012	13744.5	-0.0008	TESS
2458663.32703	0.00008	13705	-0.0016	TESS	2458679.31619	0.00008	13745	-0.0013	TESS
2458663.52658	0.00013	13705.5	-0.0019	TESS	2458679.51552	0.00013	13745.5	-0.0019	TESS
2458663.72703	0.00009	13706	-0.0014	TESS	2458679.71603	0.00009	13746	-0.0012	TESS
2458663.92646	0.00013	13706.5	-0.0018	TESS	2458679.91540	0.00012	13746.5	-0.0017	TESS
2458664.12651	0.00012	13707	-0.0016	TESS	2458680.11570	0.00008	13747	-0.0013	TESS
2458664.32607	0.00015	13707.5	-0.0019	TESS	2458680.31535	0.00012	13747.5	-0.0015	TESS
2458664.52609	0.00011	13708	-0.0017	TESS	2458680.51461	0.00007	13748	-0.0021	TESS
2458664.72592	0.00014	13708.5	-0.0018	TESS	2458680.71526	0.00011	13748.5	-0.0013	TESS
2458664.92660	0.00011	13709	-0.0009	TESS	2458680.91530	0.00006	13749	-0.0011	TESS
2458665.12564	0.00014	13709.5	-0.0018	TESS	2458681.11414	0.00011	13749.5	-0.0021	TESS
2458665.52547	0.00014	13710.5	-0.0017	TESS	2458681.31503	0.00007	13750	-0.0011	TESS
2458665.72607	0.00010	13711	-0.0009	TESS	2458681.51388	0.00011	13750.5	-0.0021	TESS
2458665.92524	0.00014	13711.5	-0.0016	TESS	2458681.71483	0.00007	13751	-0.0010	TESS
2458666.12541	0.00010	13712	-0.0013	TESS	2458681.91367	0.00011	13751.5	-0.0021	TESS
2458666.32495	0.00014	13712.5	-0.0016	TESS	2458682.11440	0.00006	13752	-0.0012	TESS
2458666.52506	0.00010	13713	-0.0014	TESS	2458682.31381	0.00011	13752.5	-0.0016	TESS
2458666.72474	0.00013	13713.5	-0.0016	TESS	2459016.08119	0.00035	14587.5	-0.0021	This study
2458666.92441	0.00009	13714	-0.0017	TESS	2459016.28093	0.00038	14588	-0.0023	This study
2458667.12463	0.00014	13714.5	-0.0014	TESS	2459016.08149	0.00030	14587.5	-0.0018	This study
2458667.32408	0.00009	13715	-0.0018	TESS	2459016.28060	0.00036	14588	-0.0026	This study
2458667.52439	0.00013	13715.5	-0.0014	TESS	2459003.09020	0.00024	14555	-0.0022	This study
2458668.92385	0.00012	13719	-0.0009	TESS	2459016.08143	0.00036	14587.5	-0.0019	This study
2458669.12343	0.00016	13719.5	-0.0012	TESS	2459016.28052	0.00036	14588	-0.0027	This study

We refined new ephemeris for this system using fitting a line on all minima times based on the MCMC method (10000 steps, 200 walkers, burn-in=100) as shown in Figure 2. We wrote this code using the emcee package in Python (Foreman-Mackey et al. 2013). The code gives changes in the light elements of the reference ephemeris as an output. We corrected reference ephemeris as

$$Min.I\ (BJD_{TDB}) = 2453185.14068(95) + 0.39972197(5) \times E\ [days] \quad (2)$$

where E is the integer number of orbital cycles after the reference epoch.

4 Binary Parameter Analysis

Analysis of the light curves to determine physical parameters of the binary system was carried out using the Wilson and Devinney (2014) code (W-D) combined with the MC simulation to reduce degeneration in the solution space and determine the uncertainties of the adjustable parameters (Zola et al. 2014,?). We set the free parameters in the MC simulation and their ranges based on previous studies of this system and the light curves obtained from our observation (Table 3).

The q-search analysis gives reliable mass ratios when full-eclipses are observed in the light curve (Kjurkchieva et al. 2019). At first, a range of fixed mass ratios from 0 to 5 was used to search. However, it only indicated minima in the range of 0.08 to 0.25 as shown in Figure 3. As a result, we found the minimum sum of the squared residuals of the W-D fit, $\sum (O-C)^2$ and $q = 0.821$. Szalai et al. (2007) determined $q = 0.82$ by a spectroscopic study on this system. Therefore, due to the close values, we fixed the 2007 study mass ratio for our final light curve solutions.

Table 3. Free parameters and search range in MC Simulations.

Parameter	Value
i (deg)	50-90
T_2 (K)	5000-7000
$\Omega_{1,2}$	1-10
l_1	1-12
q	0-5
Phase shift	-0.03-0.03
$X_{\text{Limb darkening}}$	0-1
$Y_{\text{Limb darkening}}$	0-1
co-latitude (deg)	0-180
Longitude (deg)	0-360
Spot radius (deg)	1-90
T_{spot}/T_1	0.7-1.1

Since both the primary and the secondary stars were assumed to have convective gas, gravity darkening exponents ($g_1 = g_2$) and albedos ($A_1 = A_2$) were fixed to theoretical reference values for convective gas, which are 0.32 and 0.5, respectively (Lucy 1967). Although the amount of limb darkening coefficients is considered a free parameter, the final values were in good agreement with Van Hamme (1993) tables.

According to the Phase-Flux light curve, the primary minimum is deeper but the secondary minimum happened first. The temperature of the primary star was fixed in the Szalai et al. (2007) analysis, which is the same condition as the difference in minimum deepening and the position of each minimum. We used the Gaia DR2 temperature value (5760 K) to set the temperature of the primary component.

Based on our data and after the required calibrations (Høg et al. 2000), we calculated $(B-V)_{V870\ Ara} = 0^m.632$. Thus, the effective temperature of the primary component, T_1 was assumed as 5777 K (Flower 1996). This temperature value is a good approximation because we can compare it with that of the Gaia DR2 catalog. The temperature difference is consistent; this indicates that the accuracy of the observations is reliable.

The depths of the primary and secondary minima in the light curves are different, indicating that the two stars' temperatures are not the same. As a result, we used the "overcontact binary not in thermal contact" mode. The parameters and uncertainties obtained from the light curve solutions in the BVI filters are presented in Table 4. Despite setting the range for the starpot model as free parameters (Table 3), there was need to add a hot-starspot due to the light curve solutions. Figures 4 shows our observations, TESS, and synthetic light curves.

We used the parallax from Gaia EDR3 and our photometry results for estimating absolute parameters of the binary system, and we calculated $d\,(pc) = 103.062 \pm 0.204$. According to our observation $V_{system} = 8^m.67 \pm 0.09$ and calculated $A_{d\ V} = 0.059 \pm 0.006$ (Schlafly and Finkbeiner 2011), the value of absolute magnitude, $M_{v(system)} = 3.546 \pm 0.079$, was estimated using an equation,

$$M_v = V - 5\log(d) + 5 - A_v \quad (3)$$

As our light curve solutions conclude that $l_1/l_2 = 6.273$, we calculated $M_{v(1)} = 3.707 \pm 0.072\ and\ M_{v(2)} = 5.700 \pm 0.036$. Also, with applying $(BC) = -0.022$ (Eker et al. 2020), $M_{bol(1)}$ and $M_{bol(2)}$ computed. We calculated L and R for each component of this system, using the well-known relations (Equations 4 and 5), respectively.

$$M_{bol(star)} - M_{bol(sun)} = -2.5\log\left(\frac{L_{star}}{L_{sun}}\right) \quad (4)$$

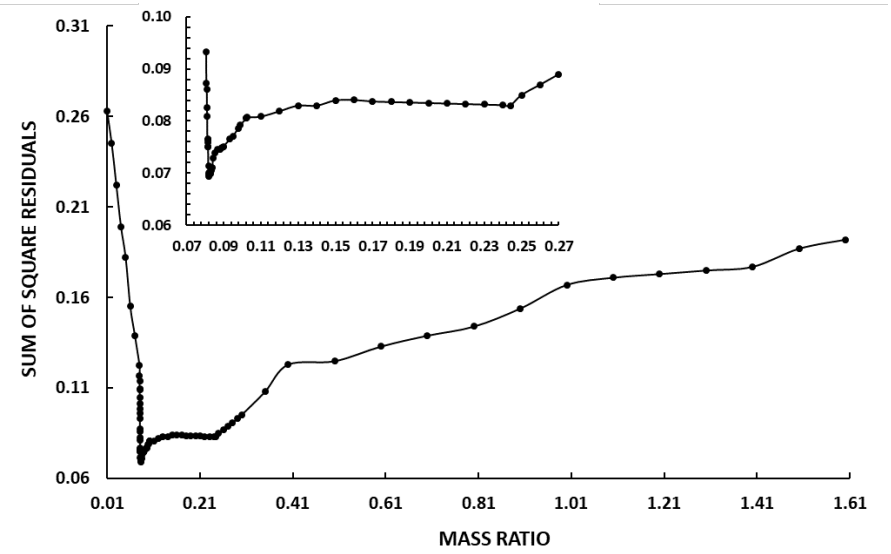

Fig. 3. Sum of the squared residuals as a function of the mass ratio. The minimum part is zoomed.

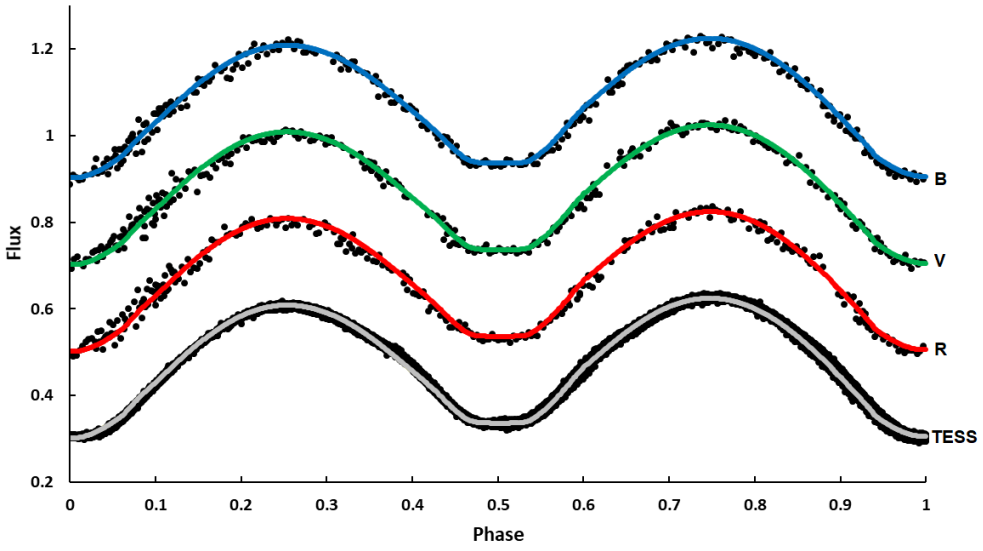

Fig. 4. Light curves from our observations and TESS (black dots). The synthetic light curves obtained from light curve solutions in the *BVI* filters and TESS are shown (top to bottom respectively); with respect to orbital phase, shifted arbitrarily in the relative flux.

$$L = 4\pi r^2 \sigma T^4 \quad (5)$$

Equation $a = R/r$ gives us a_1 and a_2, from R_1 and R_2, and also, we reckoned the average of a_1 and a_2. Finally, we calculated the masses of the components, M_1 and M_2, by Kepler's third law and our $q = (\frac{M_2}{M_1})$ value. The parameters obtained during this procedure are given in Table 5 compared to Szalai et al. (2007).

Figure 5 presents schematic representations of the two stars' relative shapes and sizes at four phases, showing their significant ellipsoidal distortion.

5 Summary and Conclusion

We obtained minimum times from new *BVI* goround-based, and TESS observations of V870 Ara using Python code. We presented a new ephemeris considering the number of minimum times during observations (2004-2020) was low. The O-C diagram shows a decrease in the orbital period that probably originated from the accumulation of measurement errors in light elements of the reference ephemeris.

Table 4. Photometric solutions of V870 Ara.

Parameter	This study
T_1 (K)	5760
T_2 (K)	5875(159)
$\Omega_1 = \Omega_2$	1.834(199)
i (deg)	73.60(64)
$q = \frac{M_2}{M_1}$	0.082
$l_1/l_{tot}(BVI)$	0.863(55)
$l_2/l_{tot}(BVI)$	0.138(55)
$l_1/l_{tot}(TESS)$	0.863(5)
$l_2/l_{tot}(TESS)$	0.138(5)
l_3	0
$A_1 = A_2$	0.50
$g_1 = g_2$	0.32
f (%)	96(4)
r_1 (mean)	0.605(4)
r_2 (mean)	0.233(4)
Colatitudespot (deg)	98
Longitudespot (deg)	84
Radiusspot (deg)	17
T_{spot}/T_{star}	1.03(1)
Phase Shift	-0.006(3)

Note: A hot-starspot is on the primary component.

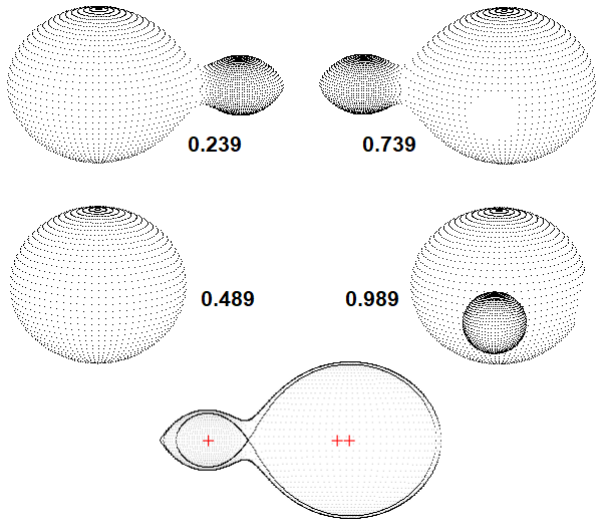

Fig. 5. The geometrical structure of V870 Ara at the four phases, and the cross-sectional outline of the binary system at the phase of 0.739 with contact degree f = 96%.

We set Gaia DR2's temperature value for the primary star, although 's $(B-V)$ value was close to this temperature. We used a mass ratio value comes from Szalai et al. (2007) study (q = 0.082), however our q-search showed almost the same value. According to the W-D code and MC simulation, it is found that V870 Ara is a contact binary with a fillout factor of f=96±4%, and an inclination of i=73.60±0.64 degrees.

We estimated the system's absolute parameters using Gaia EDR3 parallax and light curve solutions from our observations. Based on this, we obtained A_v and BC values from valid references and used the orbital period, the magnitude in V band, $l_{1,2}$, $r_{1,2(mean)}$, and mass ratio values from our calculations in this study. Therefore, the mass, radius, bolometric magnitude, and luminosity of the system were obtained. Table 5 shows that the absolute parameter values obtained in this investigation are comparable and consistent with those found in the Szalai et al. (2007) study.

According to the system's color index, the spectral type of V870 Ara is suggested as G2V from Allen's table (Cox 2000). The positions of the primary and secondary components of V870 Ara in the Mass-Radius $(M-R)$ and Mass-Luminosity $(M-L)$ diagrams on a log-scale are shown in Figure 6. These diagrams show the evolutionary status of V870 Ara.

The O'Connell effect (O'Connell 1951) can be recognized clearly in the light curves from the TESS and our observations. The most appropriate suggestion for this effect is the presence of starspot(s) induced by the components' magnetic activities (Sriram et al. 2017). The light curves of V870 Ara indicate $Max\ II$ is brighter than and $Max\ I$ asymmetry in maxima or unequal minima is clearly visible. Due to the presence of this asymmetry we used a stellar spot model during the light curve solutions. We found that assuming a hot-starspot model on the massive primary component results in an acceptable solution for all light curves.

Selam (2004) investigated the light curve solution for this binary system, reporting a mass ratio of 0.25 and a fill-out factor of 70%. This system was also studied by Szalai et al. (2007), who determined q=0.082 and f=96.4%. The orbital inclination was estimated to be 70 degrees in both studies. We fixed the mass ratio value based on the Szalai et al. (2007) study. In comparison to the previous two studies, the orbital inclination value has increased slightly. As shown by the first and second minimums of the light curves, the temperature difference between the components has decreased in our study compared to the 2007 study.

We can conclude that V870 Ara is a contact and A-type W UMa system based on the low mass ratio, large fillout factor, and temperature difference between the components. Given that the amount of evidence for a low mass ratio,

Table 5. Estimated absolute elements of V870 Ara along with the results of Szalai et al. (2007).

Parameter	This study		Szalai et al. (2007)	
	Primary	Secondary	Primary	Secondary
Mass ($M_\odot$)	1.546(54)	0.127(37)	1.503(11)	0.123(2)
Radius ($R_\odot$)	1.64(6)	0.63(5)	1.67(1)	0.61(1)
Luminosity ($L_\odot$)	2.64(17)	0.42(1)	2.96(30)	0.50(1)
M_{bol} (mag)	3.69(7)	5.68(4)	3.54(10)	5.48(10)
log g (cgs)	4.197(5)	3.943(15)	4.169(2)	3.957(7)
a ($R_\odot$)	2.71(12)		2.43(13)	

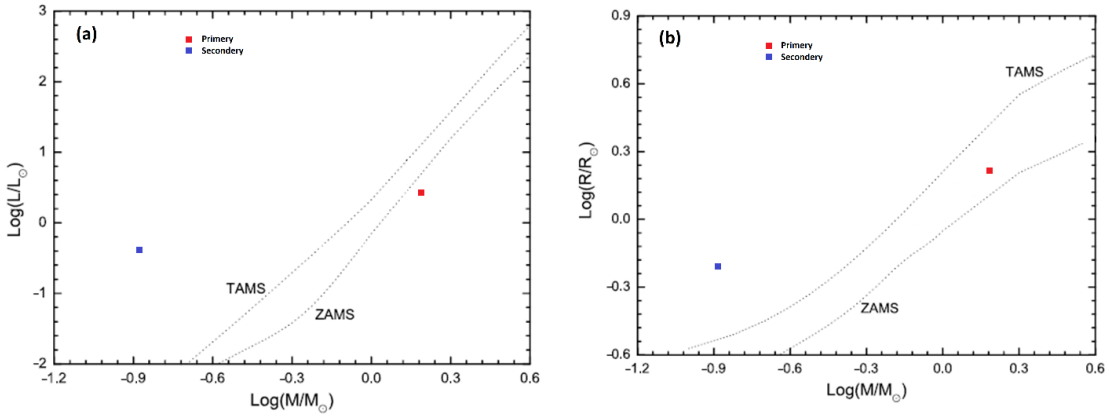

Fig. 6. The *logM* – *logR*, and *logM* – *logL* diagrams for V870 Ara from the absolute parameters.

we expect it will become a deeper contact binary based on system evolution.

Acknowledgments: This manuscript is based on the Binary Systems of South and North Project (http://bsnp.info). The project aims to study contact binary systems in the northern and southern hemispheres of several observatories in different countries. Furthermore, the authors would like to give great thanks to Dr. Fahri Alicavus for his consultations.

Author contributions: All authors contributed equally to this work.

Funding information: This project has not been sponsored by any institution.

Conflict of interest: The authors have no conflicts of interest to declare.

References

Cardoso JVDM, Hedges C, Gully-Santiago M, Saunders N, Cody AM, Barclay T, et al. **2018**. Lightkurve: Kepler and TESS time series analysis in Python. Astrophysics Source Code Library, pp.ascl-1812.

Collins KA, Kielkopf JF, Stassun KG, Hessman FV. **2017**. AstroImageJ: image processing and photometric extraction for ultra-precise astronomical light curves. AJ. 153(2):77.

Cox AN. **2000**. Allen's astrophysical quantities. Springer Verlag New York.

Eker Z, Bilir S, Yaz E, Demircan O, Helvacı M. **2009**. New absolute magnitude calibrations for WUrsa Majoris type binaries. Astron. Nachr. 330(1):68-76.

Eker Z, Soydugan F, Bilir S, Bakis V, Alicavus F, Ozer S, et al. **2020**. Empirical bolometric correction coefficients for nearby Main-Sequence Stars in Gaia era. ArXiv preprint. Available from: arXiv:2006.01836.

Flower PJ. **1996**. Transformations from theoretical Hertzsprung-Russell diagrams to color-magnitude diagrams: effective temperatures, BV colors, and bolometric corrections. ApJ. 469:355.

Foreman-Mackey D, Hogg DW, Lang D, Goodman J. **2013**. emcee: the MCMC hammer. PASP. 125(925):306.

Høg E, Fabricius C, Makarov VV, Bastian U, Schwekendiek P, Wicenec A, et al. **2000**. Construction and verification of the Tycho-2 Catalogue. A&A. 357:367-386.

Hu K, Jiang ZH, Yu YX, Xiang FY. **2018**. On orbital period changes of two low-mass-ratio and deep-contact binaries: FN Cam and KN Per. New Astron. 62:20-25.

Jenkins JM, Twicken JD, McCauliff S, Campbell J, Sanderfer D, Lung D. **2016**. The TESS science processing operations center. In: Software and Cyberinfrastructure for Astronomy IV. International Society for Optics and Photonics. 9913:99133E.

Kazarovets EV, Samus NN, Durlevich OV, Frolov MS, Antipin SV, Kireeva NN, et al. **1999**. The 74th special name-list of variable stars. Information Bulletin on Variable Stars. p. 4659.

Kjurkchieva DP, Popov VA, Petrov NI. **2019**. Global Parameters of 12 Totally Eclipsing W UMa Stars. AJ. 158(5):186.

Lucy LB. **1967**. Gravity-darkening for stars with convective envelopes. Zeitschrift fur Astrophysik. 65:89.

O'Connell DJK. **1951**. The so-called periastron effect in eclipsing binaries. MNRAS. 111(6):642-642.

Poro A, Davoudi F, Basturk O, Esmer EM, Aksaker N, Akyüz A, et al. **2020**. The first light curve solutions and Period study of BQ Ari. ArXiv preprint. Available from: arXiv:2006.00528.

Pribulla T, Rucinski SM. **2006**. Contact binaries with additional components. I. The extant data. AJ. 131(6):2986.

Salvatier J, Wiecki TV, Fonnesbeck C. **2016**. Probabilistic programming in Python using PyMC3. PeerJ Comput. Sci. 2:e55.

Selam SO. **2004**. Key parameters of W UMa-type contact binaries discovered by HIPPARCOS. A&A. 416(3):1097-1105.

Schlafly EF, Finkbeiner DP. **2011**. Measuring reddening with Sloan Digital Sky Survey stellar spectra and recalibrating SFD. ApJ. 737(2):103. DOI:https://doi.org/10.1088/0004-637X/737/2/103.

Sriram K, Malu S, Choi CS, Rao PV. **2017**. A study of the Kepler K2 variable EPIC 211957146 exhibiting a variable O'Connell effect. AJ. 153(5):231.

Szalai T, Kiss LL, Mészáros S, Vinkó J, Csizmadia S. **2007**. Physical parameters and multiplicity of five southern close eclipsing binaries. A&A. 465(3):943-952.

Ulaş B, Kalomeni B, Keskin V, Köse O, Yakut K. **2012**. Marginally low mass ratio close binary system V1191 Cyg. New Astron. 17(1):46-49.

Van Hamme W. **1993**. New limb-darkening coefficients for modeling binary star light curves. AJ. 106:2096-2117.

Wilson RE, Devinney EJ. **1971**. Realization of accurate close-binary light curves: application to MR Cygni. ApJ. 166:605.

Zola S, Gazeas K, Kreiner JM, Ogloza W, Siwak M, Koziel-Wierzbowska D., et al. **2010**. Physical parameters of components in close binary systems–VII. MNRAS. 408(1):464-474.

Zola S, Rucinski SM, Baran A, Ogloza W, Pych W, Kreiner JM, et al. **2004**. Physical parameters of components in close binary systems: III. Acta Astron. 54:299-312.